Molecular Therapy
Nucleic Acids
Brief Report

# Topical tissue nanotransfection of *Prox1* is effective in the prophylactic management of lymphedema

Ganesh Mohan,[1] Imran Khan,[1] Colby R. Neumann,[1] Miguel D. Jorge,[1] Shahnur Ahmed,[1] Luci Hulsman,[1] Mithun Sinha,[1] Gayle M. Gordillo,[1,2] Chandan K. Sen,[1,3,4] and Aladdin H. Hassanein[1,4]

[1]Department of Surgery, Indiana University School of Medicine, Indianapolis, IN, USA; [2]McGowan Institute for Regenerative Medicine, Department of Plastic Surgery, University of Pittsburgh School of Medicine, Pittsburgh, PA, USA; [3]McGowan Institute for Regenerative Medicine, Department of Surgery, University of Pittsburgh School of Medicine, Pittsburgh, PA, USA

**Lymphedema is chronic limb swelling resulting from lymphatic dysfunction. There is no cure for the disease. Clinically, a preventive surgical approach called immediate lymphatic reconstruction (ILR) has gained traction. Experimental gene-based therapeutic approaches (e.g., using viral vectors) have had limited translational applicability. Tissue nanotransfection (TNT) technology uses a direct, transcutaneous nonviral vector, gene delivery using a chip with nanochannel poration in response to a rapid (<100 ms) focused electric field. The purpose of this study was to experimentally prevent lymphedema using focal delivery of a specific gene *Prox1* (a master regulator of lymphangiogenesis). TNT was applied to the previously optimized lymphedematous mice tail (day 0) directly at the surgical site with genetic cargo loaded into the TNT reservoir: group I (sham) was given pCMV6 (expression vector backbone alone) and group II was treated with pCMV6-*Prox1*. Group II mice had decreased tail volume (47.8%) compared to sham and greater lymphatic clearance on lymphangiography. Immunohistochemistry showed greater lymphatic vessel density and RNA sequencing exhibited reduced inflammatory markers in group II compared to group I. *Prox1* prophylactically delivered using TNT to the surgical site on the day of injury decreased the manifestations of lymphedema in the murine tail model compared to control.**

## INTRODUCTION

Lymphedema is chronic limb swelling from lymphatic dysfunction, with 250 million affected people worldwide.[1] It occurs in one-third of breast cancer patients who have axillary lymph node dissection during treatment.[1,2] Fluid, adipose, and fibrosis from inflammation result in progressive limb enlargement.[3] Lymphedema affects quality of life and has a high health cost burden.[4]

Lymphedema is managed nonsurgically (compression, decongestive therapy) and surgically (excisional and microsurgical procedures).[5–7] Current treatments may variably improve limb size and symptoms but do not cure lymphedema.[5] Progressive limb enlargement from interstitial fluid retention, followed by inflammation and fibrosis over time are difficult to reverse.[5,8] A surgical approach called immediate lymphatic reconstruction (ILR) has recently emerged to prophylactically decrease the frequency of lymphedema.[9] At the time of axillary lymph node excision in breast cancer patients, disrupted afferent lymphatic vessels in the axilla are identified and microsurgically anastomosed into adjacent venules.[10] ILR can decrease the risk of acquiring lymphedema after lymphadenectomy from 30.5% to 6.6%.[10] However, access to ILR is limited because it requires specialized microsurgical training, equipment, and hospital resources.[10]

Experimental models have attempted to address the gap in management for lymphedema using gene-based strategies and proangiogenic factors.[11] Viral vector-based gene therapy or lymphangiogenesis-inducing treatments have had limited clinical translational applicability.[12] Viral vectors have raised potential oncological concern for lymphangiogenesis at unintended sites in cancer survivors who have developed lymphedema.[13] Tissue nanotransfection technology (TNT) achieves transcutaneous gene delivery using nanoelectroporation.[14] The feasibility of TNT for gene delivery has been established and validated for *in vivo* vasculogenic and neurogenic tissue reprogramming.[15,16]

Experimental therapies have primarily focused on treating animal models once lymphedema has been induced.[11] Parallel to the recent clinical focus on the prevention of lymphedema, the purpose of this investigation was to prophylactically manage lymphedema at the time of lymphatic injury in a murine tail model with focal delivery of prolymphangiogenic Prospero Homeobox 1 (*Prox1*) using TNT. Prox1 is a transcription factor that is a master switch for lymphatic

https://doi.org/10.1016/j.omtn.2024.102121.

[4]These authors contributed equally

**Correspondence:** Aladdin H. Hassanein, MD, MMSc, Department of Surgery, Indiana University School of Medicine, 545 Barnhill Dr, Suite 232, Indianapolis, IN 46202, USA.
**E-mail:** ahassane@iu.edu

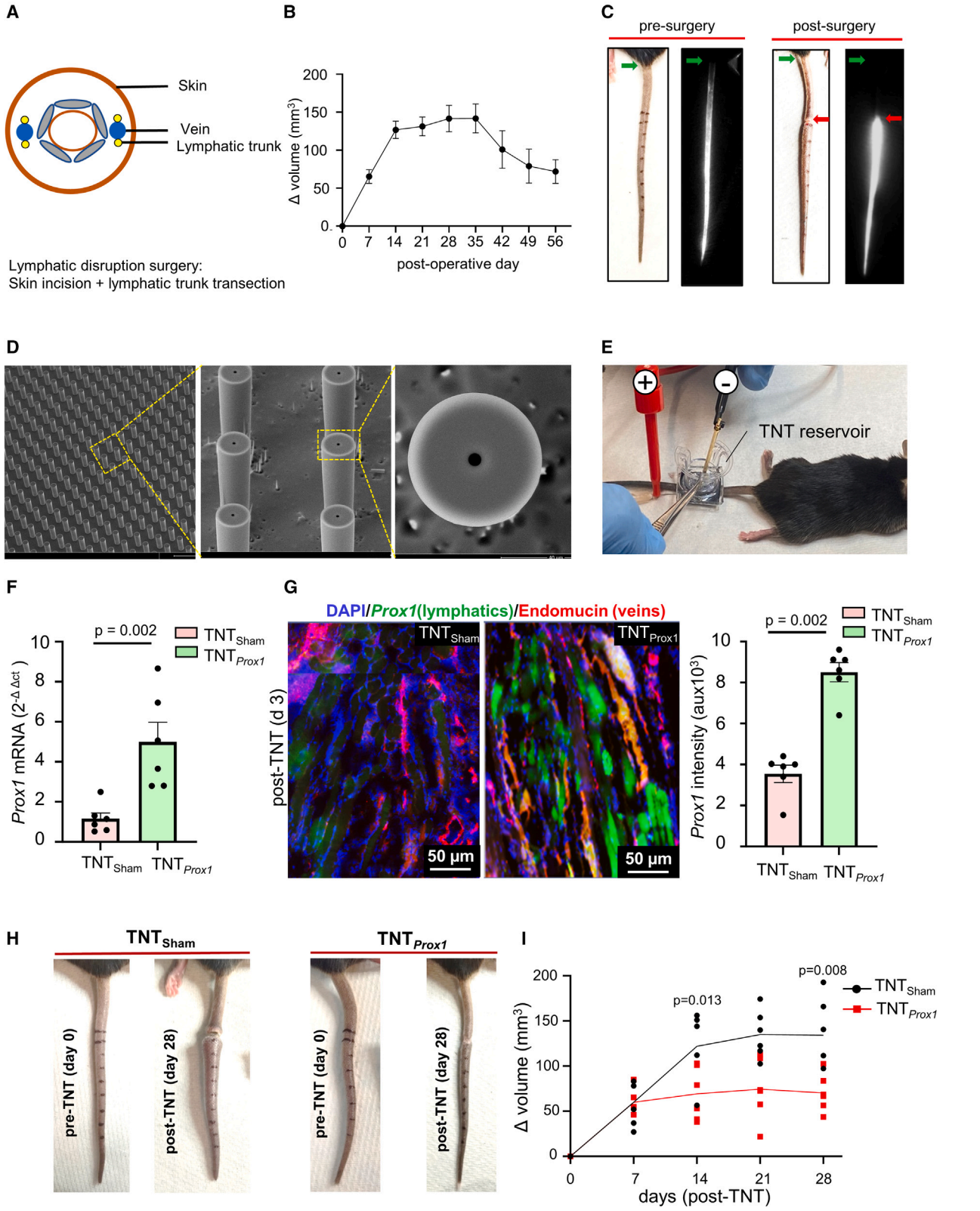


*(legend on next page)*

endothelial cell (LEC) specification, maintenance, and sprouting.[17,18] Prox1 binds to the promoter of fibroblast growth factor receptor (FRFR-3) in LECs, inducing its transcription, which supports lymphatic development.[19]

## RESULTS

### Sustained lymphatic function following TNT delivery of *Prox1* plasmid

A mouse tail model of secondary lymphedema was used by excising a 3-mm-wide skin section of the mouse tail and disconnecting the collecting lymphatic vessels. Surgical disruption of mouse tail lymphatics resulted in progressive tail swelling within the first 2 weeks (Figures 1A–1C). The model created a pathological change that mimics the obstruction of lymphatic drainage in patients. Indocyanine green (ICG) near-infrared imaging was performed to study whether lymphatic drainage was effectively blocked (Figure 1C). To help determine the efficiency of *Prox1* on lymphedema prevention, TNT-mediated focal delivery of *Prox1* was performed on the murine tail surgical site (day 0) (Figures 1D, 1E, and S1). Successful delivery and increased expression of *Prox1* in $TNT_{Prox1}$ animals was observed through qRT-PCR (3- to 4-fold) and immunohistochemistry when compared with $TNT_{Sham}$ (day 3) (Figures 1F and 1G). *Prox1* expression levels in mice tail tissue were quantified by qPCR. There was no significant difference in Prox1 mRNA transcripts between normal and lymphedematous (postoperative day 14) mice tail tissue (Figure S2). Thus, the Prox1 baseline levels were enhanced using TNT. In addition to Prox1, we also studied vascular endothelial growth factor (VegfC). $TNT_{Prox1}$ treatment significantly reduced postsurgical lymphedema by 47.8% and the $TNT_{Vegf\text{-}C}$ treatment by 34.5% when relative to $TNT_{Sham}$ (post-TNT day 28) (Figures 1H, 1I, and S3). These results demonstrate the efficiency of *Prox1* delivery through TNT and its preventive effect on lymphedema in the murine tail model.

### $TNT_{Prox1}$ improves and restores lymphatic function

A histological analysis of operated mouse tail was performed to further characterize changes of postsurgical lymphedema following TNT (day 28). Thickening of tissue has been observed in a murine tail model of lymphedema.[20] More lymphatic vessels were observed in the upper dermal layers of a mouse tail treated with $TNT_{Prox1}$ when compared to the $TNT_{Sham}$ animals as depicted through H&E and podoplanin staining (Figure S4). Tail histology revealed reduced tail edema and dermal/epidermal thickening in $TNT_{Prox1}$ compared to $TNT_{Sham}$ group, 4 weeks postsurgery (Figures 2A, 2B, and S5A–S5D). Lymphedema results in tissue fibrosis mediated by increased collagen deposition. We quantified collagen density by measuring the percentage of picrosirius red–stained dermis (Figures S5E–S5H). Reduced (13%) picrosirius red staining was observed in $TNT_{Prox1}$ compared to the $TNT_{\mathbf{Sham}}$ group, indicating a reduced fibrotic response to lymphedema in the $TNT_{Prox1}$ cohort (Figure 2C). Immunohistochemistry staining (molecular assessment) exhibited an increased abundance of lymphatic endothelial-specific marker (podoplanin and Prox1) in $TNT_{Prox1}$ animals (Figures 2D and S6) and significant reduction of the tissue area covered by lymphatic vessels (Lyve1) (Figure 2E). ICG lymphangiography (functional assessment) was carried out at postoperative day 28 on $TNT_{Sham}$ versus $TNT_{Prox1}$ group. At day 28 (post-TNT), the relative mice tail volume of the $TNT_{Sham}$ animals remained significantly increased relative to $TNT_{Prox1}$ animals. It was observed that $TNT_{Sham}$ animals had a consistent fluorescent signal for up to 96 h when compared with $TNT_{Prox1}$. ICG clearance was significantly faster in the $TNT_{Prox1}$ animals at 48, 72, and 96 h, indicating improved lymphatic clearance (Figures 2F and 2G).

### $TNT_{Prox1}$ reduces lymphedema-associated inflammation

Lymphedema tissue exhibits upregulated inflammatory genes similar to that found in acute inflammation.[20] Inflammatory response after lymphatic dysfunction results in soft tissue fibrosis and adipose deposition.[8,21] Comprehensive transcriptomic analyses using bulk RNA sequencing (RNA-seq) revealed a reduced abundance of genes involved in the inflammatory pathway in the $TNT_{Prox1}$ compared to the $TNT_{\mathbf{Sham}}$ group 4 weeks postsurgery (Figures 3A and 3B). The $TNT_{Prox1}$ cohort also exhibited a reduced abundance of $CD4^+$ T cells, indicative of faster resolution or reduced infiltration of inflammatory immune cells (Figure 3B). In addition, volcano plot gene enrichment shows the differential gene expression between two groups ($TNT_{Sham}$ versus $TNT_{Prox1}$) (Figure S7). Downregulation of *Ccl1* (involved with T cell response) and miR-146b (microRNA [miR] associated with inflammatory response) was observed in the $TNT_{Prox1}$ cohort (Figures 3C and 3D). In addition, the downregulation of *Ccr4*, *Ccl27*, *Tac1* and others was noted (Figures 3C and 3D). *Tac1* is a member of Tachykinin family. It is associated with the inflammatory pain response.[22] Also, the reduced lipid content (perilipin staining) (Figure 3E) and increased proliferating lymphatic endothelial marker (Ki67 staining) were observed in $TNT_{Prox1}$ animals (Figure 3F).

**Figure 1. Preventive therapy with $TNT_{Prox1}$ to minimize lymphedema progression**

(A) Schematic representation of mouse tail model of acquired lymphedema surgically induced in the tails of C57BL/6 mice through transection of lymphatic trunks. (B) Natural progression of mouse tail model of lymphedema. Change in tail volume over a period of 56 days measured using truncated cone equation. (C) Blockage of lymphatic trunk postsurgery validated through near-infrared imaging of tail using ICG dye. The green arrows mark the base of the tail, and the red arrow marks the site of lymphatic transection. (D) Scanning electron microscopy of $TNT_{2.0}$ showing the nanoneedles and pore diameter of 3.9 μm. (E) Topical delivery of pCMV6-*Prox1* using $TNT_{2.0}$ in mice tail model on the day of surgery (day 0). The positive and negative electrical probes are attached, and a brief square wave pulse electric stimulation is delivered (10 × 10-ms pulses, 250 V, 10 mA) facilitating focal, nonviral, transcutaneous transfection. (F and G) Validation of TNT-mediated pCMV6-*Prox1* delivery and expression through (F) qRT-PCR and (G) immunostaining with anti-Prox1 antibody using $TNT_{2.0}$. Mean ± SEM. (H and I) Prevention of lymphedema progression following $TNT_{Prox1}$ compared to $TNT_{sham}$. (H) Representative image of the murine tail in 2 groups at days 0 and 28 following TNT. (I) Comparative line graph of 2 groups $TNT_{Prox1}$ (red) and $TNT_{sham}$ (black). $TNT_{Sham}$ versus $TNT_{Prox1}$ (day 14, $p = 0.013$) and (day 28, $p = 0.008$). The Mann-Whitney test was performed for statistical analysis to compare $TNT_{Sham}$ versus $TNT_{Prox1}$. $p < 0.05$ is considered as statistally significant.

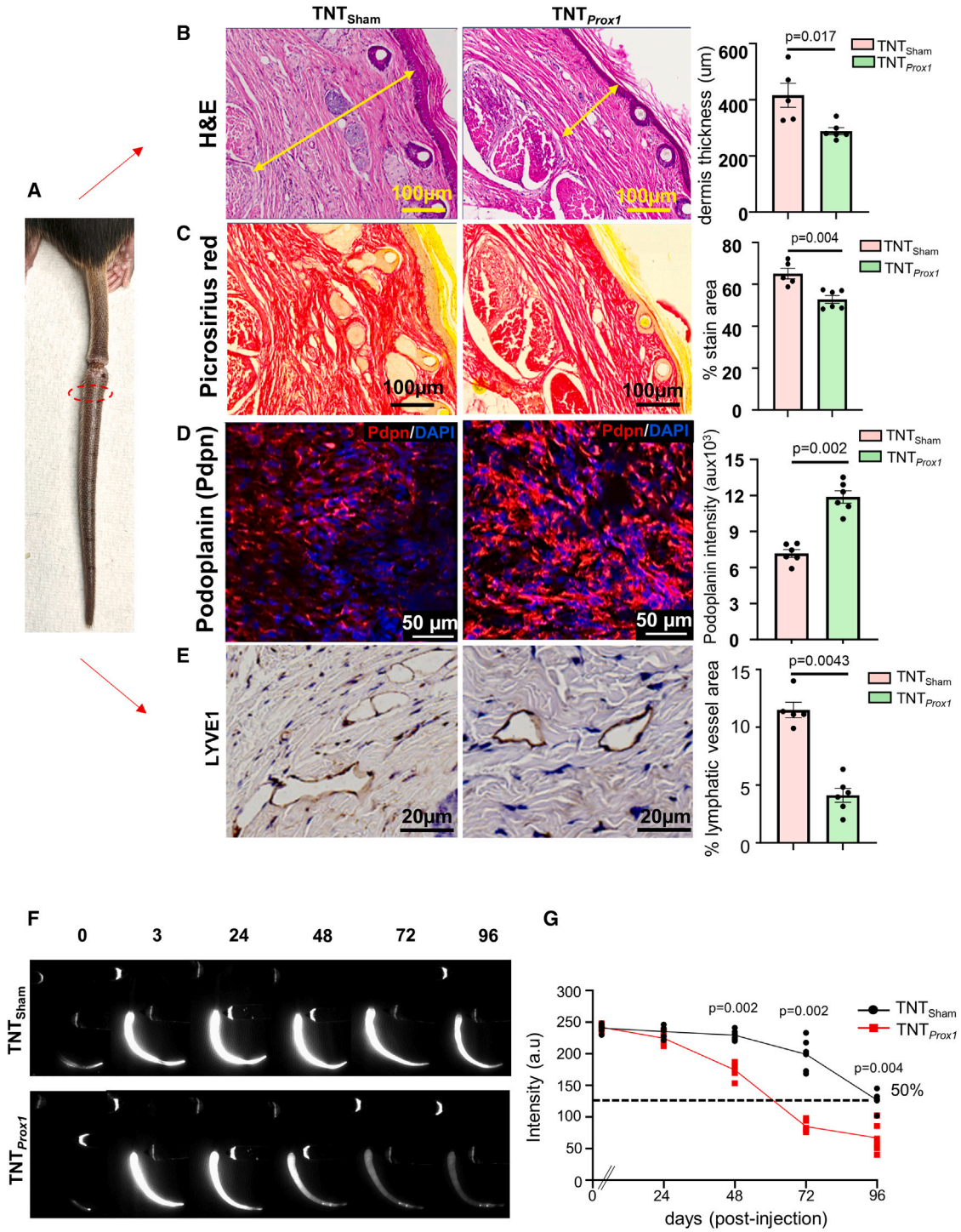


**Figure 2. TNT$_{Prox1}$ improves tail anatomy and lymphatic function**

(A) Lymphedema-induced murine tail. The red circle indicates the site distal to lymphatic transection surgery used for histological analyses. (B and C) Histological analyses of lymphedema-induced murine tail cross-sections at post-TNT day 28. (B) Dermal thickening analyses by H&E staining. Mean dermal thickness in mice tail skin is significantly less in TNT$_{Prox1}$ animals when compared to TNT$_{Sham}$ ($p = 0.017$) cohort. (C) Collagen deposition analyses by picrosirius red staining. Reduced abundance of collagen deposition in the TNT$_{Prox1}$ animals when compared to TNT$_{Sham}$ ($p = 0.004$). (D) Increased expression of lymphatic marker podoplanin (Pdpn) as quantified using immunochemistry with antipodoplanin (red) in mice tail (post-TNT day 28). (E) Improvement in lymphatic dilation (i.e., restoration of lymphatic structure) in TNT$_{Prox1}$ animals when

*(legend continued on next page)*

## DISCUSSION

Lymphedema is a challenging problem and difficult to reverse. Thus, prevention of lymphedema has become a recent area of emphasis, such as with microsurgical lymphovenous anastomosis of disrupted axillary lymphatics during axillary dissection.[23] We demonstrate the first report of the prophylactic management of lymphedema using a TNT-based approach for gene delivery. Other investigators have used intraperitoneal/drug depot of 9-*cis* retinoic acid, *Vegf-C* mRNA-lipid nanoparticles and tacrolimus to minimize lymphedema in a mouse model.[24–26] Nonviral, focal TNT delivery can address the concerns of global prolymphangiogenic genes promoting tumor recurrence in postcancer lymphedema.[27,28] The results of *Prox1* delivery with TNT demonstrate an effective, novel, focal nanotechnology approach for genetic cargo delivery in the murine tail lymphedema model to prevent lymphedema.

Lymphedema does not reduce the expression of Prox1. As exhibited in the results, there was no significant difference in *Prox1* mRNA transcripts between normal and lymphedematous mice tail tissue on postoperative day 14. Hence, delivery of *Prox1* through TNT increases the basal level of Prox1 and increases lymphangiogenesis. Although TNT was able to be used to topically deliver *Prox1* in the mouse tail model and limit lymphedema, precise penetration depth is necessary for efficacy. TNT is focal and nonsystemic; therefore, the depth of local delivery transcutaneously must reach the intended cells. A previous study[14] reported that the depth of penetration of fluorescently labeled fluorescein amidite-DNA (FAM-DNA) can be controlled by adjusting the voltage of the electrical pulse. In our previous report,[28] we demonstrated that the delivery of genetic cargo (FAM-labeled DNA) in the murine tail lymphedema model using TNT had a depth of transfection of ~800–1000 μm. Although this was effective in the mouse tail model of lymphedema, human skin is multilayered, with variable thickness and conduction properties.[29] Exfoliation has been shown to enhance TNT delivery.[29] In a potential clinical application in lymph node dissection, an open wound for surgical access would allow for direct transfection to the disrupted lymphatics.

After validation of TNT for focal gene delivery in the murine tail lymphedema model, we further compared the TNT treatment of *Prox1* and *Vegf-C* in the mouse tail lymphedema model. The reduction in lymphedema swelling occurred more through *Prox1* delivery as compared to *VegfC*. This could be due to the fact that Prox1 is a master regulator of lymphangiogenesis and sits upstream in lymphatic development compared to VegfC, which is downstream and involved in lymphatic maturation. Hence, we have focused on $TNT_{Prox1}$ in this study. We showed that *Prox1* prevented the development of chronic lymphedematous skin changes, with animals exhibiting reduced fibrosis, lipid accumulation, and collagen compared to $TNT_{Sham}$. Histology revealed an increased abundance of lymphatic molecular marker podoplanin and Prox1 in $TNT_{Prox1}$ animals. This greater lymphatic density indicates lymphangiogenesis, which may permit lymphatic fluid to drain faster in the $TNT_{Prox1}$ animal. In addition, RNA-seq and qPCR analysis revealed reduced inflammatory response in the $TNT_{Prox1}$ animals when compared to the $TNT_{Sham}$ animals. Overall, the *Prox1* prevented the secondary changes associated with the postsurgical lymphedema.

In summary, we present a feasible method of gene therapy for the prevention of postsurgical lymphedema. There is high clinical translational applicability with focal and *in situ* delivery of lymphangiogenic factors to lymphedema severity by promoting functional neolymphangiogenesis. This mode of therapeutic management could facilitate disease prevention and avoid the inflammatory cascade of chronic lymphedema, which is difficult to reverse.

## MATERIALS AND METHODS

### Animals

All of the animal (mice) experiments were performed in accordance with protocol 22020 approved by the Indiana University School of Medicine Institutional Animal Care and Use Committee. Animals were maintained under a 12-h light:dark cycle with *ad libitum* access to food and water.

### Surgical disruption of mouse tail lymphatics

Acquired lymphedema was surgically induced in the tails of C57BL/6 mice through lymphatic surgery, using a protocol that has been previously developed[20] and optimized.[28] Under isoflurane-inhaled anesthesia (2%), a 3-mm full-thickness skin excision was performed in the murine tail 2 cm from the base. Methylene blue (0.1 mL) was injected into the distal portion of the tail to facilitate the identification of lymphatics. Using a surgical microscope, the lymphatic vessels adjacent to the lateral veins in the tail were localized and transected. The underlying bone, muscle, major blood vessels, and tendons were left intact.

### TNT for *in vivo* reprogramming

A murine tail lymphedema model was used to deliver the *Prox1* and *VegfC* through TNT. TNT was performed immediately after the surgical disruption of lymphatics on mice tails. The TNT device was used as described previously.[27] TNT was applied in a tangential contact point at the surgical site and distal regions of the mouse tail (Figure S1).

The skin was exfoliated at the distal region of the tail to eliminate the dead/keratin cell layers to expose nucleated cells in the epidermis. *Prox1*/*Vegf-C* plasmid cocktail was loaded in the

compared to $TNT_{Sham}$. Representative Lyve1-stained cross-section of operated mice tail post-TNT day 28. (F and G) Faster resolution of fluorescent dye injected in interstitial space of tail tip in $TNT_{Prox1}$ cohort when compared to $TNT_{Sham}$. Representative photographs from near-infrared imaging of murine tail (F) and fluorescence (in arbitrary units) were plotted as a function of time (G). The collecting lymphatic function was tracked by imaging the clearance of ICG dye in the vessels on post-TNT day 28. Time-lapse images were captured for 96 h postinjection. Mean ± SEM. The Mann-Whitney test was performed for statistical analysis to compare $TNT_{Sham}$ versus $TNT_{Prox1}$. $p < 0.05$ is considered as statistally significant.

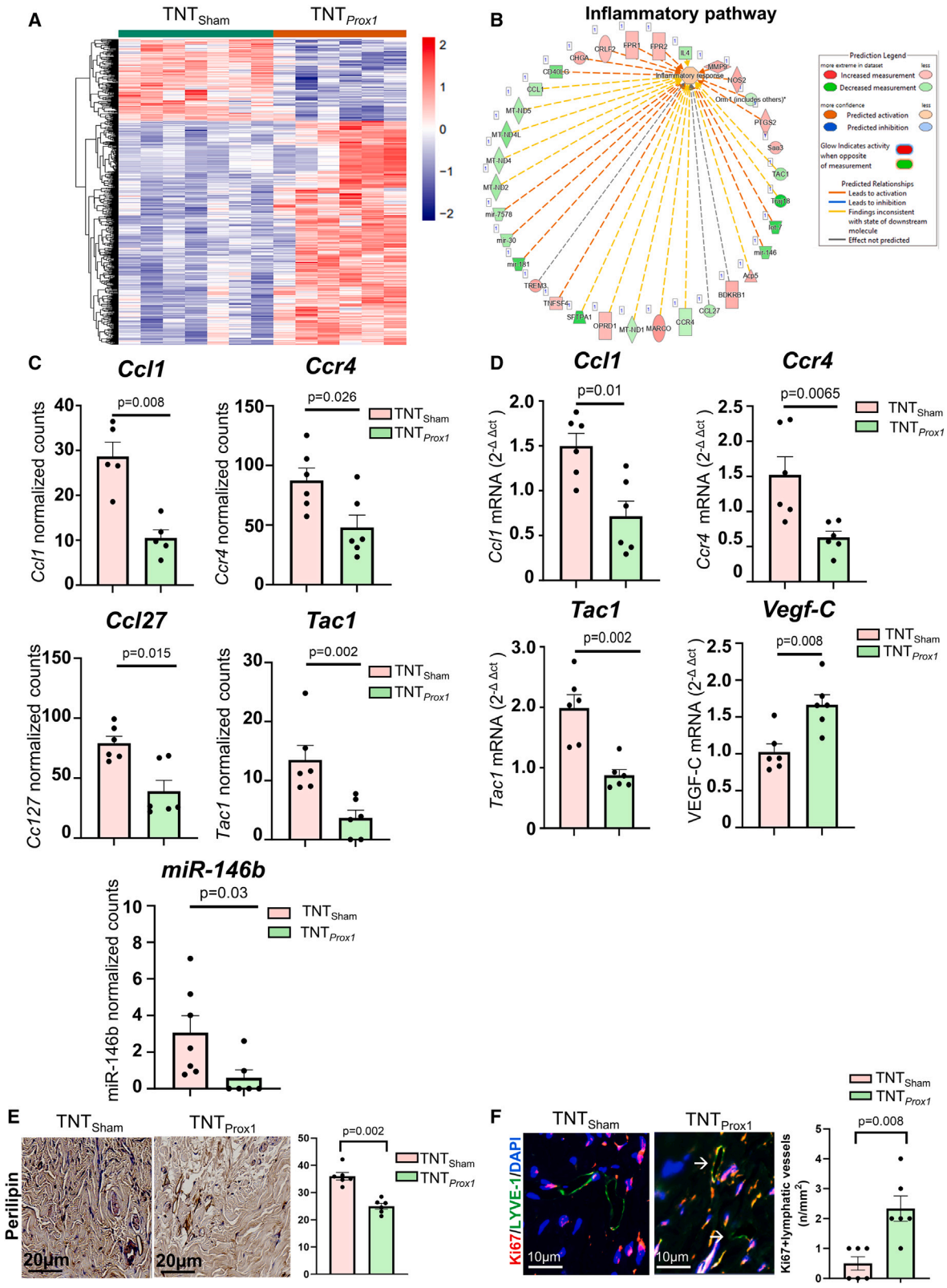


*(legend on next page)*

reservoir at a concentration of 0.05–0.1 μg $\mu L^{-1}$. A gold-coated electrode (cathode) was immersed in the plasmid solution, and a 30G needle counterelectrode (anode) was inserted into the dermis below the tail juxtaposed to the TNT platform surface. TNT was applied to the murine tail (day 0) directly at the occlusion site and distal region, with genetic cargo loaded into the TNT reservoir: group I (control) was given pCMV6 (expression vector backbone alone) (n = 6); group II was given pCMV6-*Prox1*/*Vegf-C* (n = 6). TNT was applied with square wave pulse electric stimulation (10 × 10-ms pulses, 250 V, 10 mA).

### Mouse tail volume quantification

Mouse tail volume quantification was performed before and after the lymphatic disruption surgery at regular intervals. The mouse tail diameter was measured at 5-mm increments starting 20 mm from the base of the tail using a digital caliper. These tail measurements were used to calculate the volume using the truncated cone equation.[30] Mice tail images were captured at regular intervals with a fixed distance.

### Histological procedures and immunostaining

After 72 h of $TNT_{Prox1}$, the mouse tail was collected from proximal, occlusion, and distal sites and stored in optimal cutting temperature (OCT) medium to validate the delivery and expression of *Prox1*. To monitor the proliferation of the lymphatic vessels and assessment of postsurgical lymphedema, immunohistochemistry was performed post-TNT (day 28) on the distal region of the mouse tail. Mice tail tissue harvested at euthanasia was fixed in 10% neutral buffered formalin, decalcified, embedded in paraffin, and sectioned in 3- to 5-μm intervals. Samples were stained with H&E using standard techniques. Picrosirius red staining was performed by bathing cross-sections in picrosirius red solution for 40 min, followed by dehydration and mounting. Immunohistochemical staining of the sections was performed using standard procedures with the following primary antibodies: α-Prox1 antibody (ThermoFisher, catalog no. PA526170; dilution; 1:100), α-podoplanin (Abcam, catalog no. ab92319; dilution 0.2:100), α-endomucin (Abcam, catalog no. ab106100; dilution 1:200), α-LYVE-1 (R&D Systems, catalog no. AF2125), α-Ki67 (Abcam, catalog no. ab16667), and α-perilipin (Abcam, catalog no. ab61682; dilution 1:200). To enable fluorescence detection, sections were incubated with appropriate Alexa Fluor 488 (green, Molecular Probes), or Alexa Fluor 564 (red, Molecular Probes)-conjugated secondary antibodies. For 3,3-diaminobenzidine (DAB) staining, the slides were incubated with horseradish peroxidase–conjugated rabbit/goat immunoglobulin G for 1 h at 37°C, followed by staining with DAB and H&E. Cells coexpressing brown (DAB) and blue (nucleus) colors were considered for analyses. Images were collected using an Axio Scan.Z1 (Zeiss). The image analysis software Zen (Zeiss) was used to quantitate fluorescence intensity. Detailed key resources are provided in Table S1.

### qRT-PCR

Mouse tail tissue was pulverized using tissue pulverizer (6770 Freezer/Mill), and total RNA was extracted using the NucleoSpin RNA kit (Macherey-Nagel). cDNA was made using SuperScript VILO cDNA Synthesis Kit (Invitrogen). The quantitative or real-time PCR (SYBR Green) approach was used for mRNA quantification. The primer sequences used in this study are provided in Table S2.

### ICG lymphangiography

ICG lymphangiography was adapted from techniques previously described for mice hindlimbs.[24] Briefly, anesthetized mice were administered 10-μL subdermal injections of 2.5 mg/mL ICG (LUNA) into the distal region of the tail. Fluorescence imaging was recorded using the SPY device (Stryker). ICG clearance was evaluated by plotting the fluorescence intensity as a function of time.

### RNA-seq

RNA-seq was performed on total RNA extracted from mouse tail tissue. Sequencing reads were covered at 50 million.

#### *RNA extraction*

Homogenization of the tissue was done with Bead Bug 6 homogenizer (Benchmark Scientific) in a cold room. Frozen tissue cores were transferred into 2-mL prefilled tubes containing 3-mm zirconium beads (Benchmark Scientific, catalog no. D1032-30), 350-μL RLT Lysis Buffer (from the kit), and 2-mercaptoethanol per kit instructions. Homogenization conditions: 4,000 rpm for 45 s was repeated 2 times with 90-s rest time between repeats. The extraction process was completed per the kit instructions. RNA was eluted with 30 μL RNase-free water.

#### *Library preparation*

The bulk RNA-seq libraries were generated using the TruSeq Stranded mRNA kit protocol. In brief, the integrity of the RNA was checked with the Agilent Tape station. The mRNA was purified

**Figure 3. $TNT_{Prox1}$ reduces lymphedema-associated inflammation and lipid content and promotes the proliferation of LECs in mice**

(A) $TNT_{Prox1}$ resulted in changed transcriptome profile exhibited in mouse tails via hierarchical clustering of differentially expressed genes and controlled by false discovery rate < 0.05 of $TNT_{Sham}$ and $TNT_{Prox1}$. (B) Reduced abundance of transcripts in the inflammatory pathway following $TNT_{Prox1}$ compared to $TNT_{Sham}$. The canonical pathway for inflammatory response was used to compare the differential expressed genes between the 2 cohorts. (C) RNA-seq analyses–based reduction of inflammatory responsive genes and miRs. *Ccl1*, *Ccr4*, *Ccl27*, *Tac1*, and miR-146b in $TNT_{Prox1}$ compared to $TNT_{Sham}$. (D) Decreased expression of inflammatory responsive genes *Ccl1*, *Ccr4*, and *Tac1* in $TNT_{Prox1}$ as measured by quantitative real-time PCR compared with $TNT_{Sham}$. Increased expression of lymphangiogenic gene *Vegf-C* was observed in $TNT_{Prox1}$ compared to $TNT_{Sham}$. RNA quantity was expressed relative to the corresponding β-actin. (E) Decreased lipid content was observed in $TNT_{Prox1}$ as measured by perilipin expression levels through immunohistochemistry compared to $TNT_{Sham}$. (F) Increased proliferation of cells as exhibited via Ki67 staining in lymphatic lumens co-stained with lymphatic marker Lyve1 in the $TNT_{Prox1}$ cohort compared to $TNT_{Sham}$. Mean ± SEM. The Mann-Whitney test was performed for statistical analysis to compare $TNT_{Sham}$ versus $TNT_{Prox1}$. $p < 0.05$ is considered as statistally significant.

from 1 μg of total RNA for each sample. After cDNA synthesis and adapter ligation, the library was amplified with 12 rounds of PCR. Bioinformatic analyses were performed (details in supplemental information). The RNA-Seq data have been deposited in the NCBI Gene Expression Omnibus (accession# GSE214301).

#### Quantification and statistical analysis

Samples were coded, and data collection was performed in a blinded fashion. Data are reported as mean ± SE of 6–8 biological replicates. Failed transfections (e.g., due to poor contact between the skin and the nanochannels, or nanochannel clogging) were omitted from the analysis. Statistical differences were determined using parametric/nonparametric tests, as appropriate, with GraphPad Prism version 9. The Mann-Whitney test was performed.

## DATA AND CODE AVAILABILITY

RNA-seq data are available in the NCBI Gene Expression Omnibus (GEO: GSE214301).

## SUPPLEMENTAL INFORMATION

Supplemental information can be found online at https://doi.org/10.1016/j.omtn.2024.102121.

## ACKNOWLEDGMENTS

This work was supported by the US Department of Defense (W81XWH2110135), the National Institutes of Health grants R21AR082600 and K08HL167164 (to A.H.H.), The Plastic Surgery Foundation, the American Association of Plastic Surgeons, and the Indiana Clinical and Translational Sciences Institute grants to A.H.H. The content is solely the responsibility of the authors and does not necessarily represent the official views of the National Institutes of Health or other sponsors. We thank the Center for Genomics and Bioinformatics at Indiana University (IU), Bloomington, for their assistance with the RNA-seq experiments. Histology services were provided by the Histology and Histomorphometry Core at the IU Musculoskeletal Health Center.

## AUTHOR CONTRIBUTIONS

A.H.H., M.S. and C.K.S. conceived and designed the work. G.M., I.K., C.R.N., M.D.J., M.S., S.A., L.H., and A.H.H. participated in the data acquisition and analyses. A.H.H., G.M., M.S., and C.K.S. wrote the manuscript. A.H.H., M.S., G.M.G., and C.K.S. reviewed the manuscript.

## DECLARATION OF INTERESTS

The authors declare no competing interests.

## REFERENCES

1. Schulze, H., Nacke, M., Gutenbrunner, C., and Hadamitzky, C. (2018). Worldwide assessment of healthcare personnel dealing with lymphoedema. Health Econ. Rev. *8*, 10.
2. Soran, A., D'Angelo, G., Begovic, M., Ardic, F., Harlak, A., Samuel Wieand, H., Vogel, V.G., and Johnson, R.R. (2006). Breast cancer-related lymphedema–what are the significant predictors and how they affect the severity of lymphedema? Breast J. *12*, 536–543.
3. Azhar, S.H., Lim, H.Y., Tan, B.K., and Angeli, V. (2020). The Unresolved Pathophysiology of Lymphedema. Front. Physiol. *11*, 137.
4. Bundred, N., Foden, P., Todd, C., Morris, J., Watterson, D., Purushotham, A., Bramley, M., Riches, K., Hodgkiss, T., Evans, A., et al. (2020). Increases in arm volume predict lymphoedema and quality of life deficits after axillary surgery: a prospective cohort study. Br. J. Cancer *123*, 17–25.
5. Carl, H.M., Walia, G., Bello, R., Clarke-Pearson, E., Hassanein, A.H., Cho, B., Pedreira, R., and Sacks, J.M. (2017). Systematic Review of the Surgical Treatment of Extremity Lymphedema. J. Reconstr. Microsurg. *33*, 412–425.
6. Hassanein, A.H., Danforth, R., DeBrock, W., Mailey, B., Lester, M., and Socas, J. (2020). Deep Inferior Epigastric Artery Vascularized Lymph Node Transfer: A Simple and Safe Option for Lymphedema. J. Plast. Reconstr. Aesthetic Surg. *73*, 1897–1916.
7. Imai, H., Kawase, T., Yoshida, S., Mese, T., Roh, S., Fujita, A., Uchiki, T., Sasaki, A., Nagamatsu, S., Takazawa, A., et al. (2023). Peripheral T cell profiling reveals downregulated exhaustion marker and increased diversity in lymphedema post-lymphatic venous anastomosis. iScience *26*, 106822.
8. Ghanta, S., Cuzzone, D.A., Torrisi, J.S., Albano, N.J., Joseph, W.J., Savetsky, I.L., Gardenier, J.C., Chang, D., Zampell, J.C., and Mehrara, B.J. (2015). Regulation of inflammation and fibrosis by macrophages in lymphedema. Am. J. Physiol. Heart Circ. Physiol. *308*, H1065–H1077.
9. Cook, J.A., Sasor, S.E., Loewenstein, S.N., DeBrock, W., Lester, M., Socas, J., Ludwig, K.K., Fisher, C.S., and Hassanein, A.H. (2021). Immediate Lymphatic Reconstruction after Axillary Lymphadenectomy: A Single-Institution Early Experience. Ann. Surg Oncol. *28*, 1381–1387.
10. Cook, J.A., Sinha, M., Lester, M., Fisher, C.S., Sen, C.K., and Hassanein, A.H. (2022). Immediate Lymphatic Reconstruction to Prevent Breast Cancer-Related Lymphedema: A Systematic Review. Adv. Wound Care *11*, 382–391.
11. Brown, S., Dayan, J.H., Coriddi, M., Campbell, A., Kuonqui, K., Shin, J., Park, H.J., Mehrara, B.J., and Kataru, R.P. (2022). Pharmacological Treatment of Secondary Lymphedema. Front. Pharmacol. *13*, 828513.
12. Marx, V. (2015). Cell biology: delivering tough cargo into cells. Nat. Methods *13*, 37–40.
13. Lee, A.S., Tang, C., Rao, M.S., Weissman, I.L., and Wu, J.C. (2013). Tumorigenicity as a Clinical Hurdle for Pluripotent Stem Cell Therapies. Nat. Med. *19*, 998–1004.
14. Xuan, Y., Ghatak, S., Clark, A., Li, Z., Khanna, S., Pak, D., Agarwal, M., Roy, S., Duda, P., and Sen, C.K. (2021). Fabrication and use of silicon hollow-needle arrays to achieve tissue nanotransfection in mouse tissue *in vivo*. Nat. Protoc. *16*, 5707–5738.
15. Gordillo, G.M., Guda, P.R., Singh, K., Biswas, A., Abouhashem, A.S., Rustagi, Y., Sen, A., Kumar, M., Das, A., Ghatak, S., et al. (2023). Tissue nanotransfection causes tumor regression by its effect on nanovesicle cargo that alters microenvironmental macrophage state. Mol. Ther. *31*, 1402–1417.
16. Ghatak, S., Khanna, S., Roy, S., Thirunavukkarasu, M., Pradeep, S.R., Wulff, B.C., EL Masry, M.S., Sharma, A., Palakurti, R., Ghosh, N., et al. (2023). Driving adult tissue repair via re-engagement of a pathway required for fetal healing. Mol. Ther. *31*, 454–470.
17. Bui, K., and Hong, Y.K. (2020). Ras Pathways on Prox1 and Lymphangiogenesis: Insights for Therapeutics. Front. Cardiovasc. Med. *7*, 597374.
18. Wigle, J.T., Harvey, N., Detmar, M., Lagutina, I., Grosveld, G., Gunn, M.D., Jackson, D.G., and Oliver, G. (2002). An essential role for Prox1 in the induction of the lymphatic endothelial cell phenotype. EMBO J. *21*, 1505–1513.
19. Shin, J.W., Min, M., Larrieu-Lahargue, F., Canron, X., Kunstfeld, R., Nguyen, L., Henderson, J.E., Bikfalvi, A., Detmar, M., and Hong, Y.K. (2006). Prox1 promotes lineage-specific expression of fibroblast growth factor (FGF) receptor-3 in lymphatic endothelium: A role for FGF signaling in lymphangiogenesis. Mol. Biol. Cell *17*, 576–584.
20. Tabibiazar, R., Cheung, L., Han, J., Swanson, J., Beilhack, A., An, A., Dadras, S.S., Rockson, N., Joshi, S., Wagner, R., and Rockson, S.G. (2006). Inflammatory manifestations of experimental lymphatic insufficiency. PLoS Med. *3*, e254.
21. Avraham, T., Zampell, J.C., Yan, A., Elhadad, S., Weitman, E.S., Rockson, S.G., Bromberg, J., and Mehrara, B.J. (2013). Th2 differentiation is necessary for soft tissue

fibrosis and lymphatic dysfunction resulting from lymphedema. FASEB J *27*, 1114–1126.

22. Shanley, L., Lear, M., Davidson, S., Ross, R., and MacKenzie, A. (2011). Evidence for regulatory diversity and auto-regulation at the TAC1 locus in sensory neurones. J. Neuroinflammation *8*, 10.
23. Cook, J.A., and Hassanein, A.H. (2021). ASO Author Reflections: Immediate Lymphatic Reconstruction: A Proactive Approach to Breast Cancer-Related Lymphedema. Ann. Surg Oncol. *28*, 1388–1389.
24. Bramos, A., Perrault, D., Yang, S., Jung, E., Hong, Y.K., and Wong, A.K. (2016). Prevention of Postsurgical Lymphedema by 9-cis Retinoic Acid. Ann. Surg. *264*, 353–361.
25. Gardenier, J.C., Kataru, R.P., Hespe, G.E., Savetsky, I.L., Torrisi, J.S., Nores, G.D.G., Jowhar, D.K., Nitti, M.D., Schofield, R.C., Carlow, D.C., and Mehrara, B.J. (2017). Topical tacrolimus for the treatment of secondary lymphedema. Nat. Commun. *8*, 14345.
26. Szőke, D., Kovács, G., Kemecsei, É., Bálint, L., Szoták-Ajtay, K., Aradi, P., Styevkóné Dinnyés, A., Mui, B.L., Tam, Y.K., Madden, T.D., et al. (2021). Nucleoside-modified VEGFC mRNA induces organ-specific lymphatic growth and reverses experimental lymphedema. Nat. Commun. *12*, 3460.
27. Gallego-Perez, D., Pal, D., Ghatak, S., Malkoc, V., Higuita-Castro, N., Gnyawali, S., Chang, L., Liao, W.C., Shi, J., Sinha, M., et al. (2017). Topical tissue nano-transfection mediates non-viral stroma reprogramming and rescue. Nat. Nanotechnol. *12*, 974–979.
28. Hassanein, A.H., Sinha, M., Neumann, C.R., Mohan, G., Khan, I., and Sen, C.K. (2021). A Murine Tail Lymphedema Model. J. Vis. Exp. *168*.
29. Li, Z., Xuan, Y., Ghatak, S., Guda, P.R., Roy, S., and Sen, C.K. (2022). Modeling the gene delivery process of the needle array-based tissue nanotransfection. Nano Res. *15*, 3409–3421.
30. Sitzia, J. (1995). Volume measurement in lymphoedema treatment: examination of formulae. Eur. J. Cancer Care *4*, 11–16.